CHAPTER II

THEORETICAL BACKGROUND OF GaAsN ALLOY SEMICONDUCTOR

The characteristic properties of the GaAsN alloy system are explained in this chapter. It consists of two main parts: the physical parameters (lattice constant, fundamental electronic band structure and strain) of GaAsN alloy film (bulk layer) and GaAsN/GaAs QWs which include quantum confinement, effective mass and band alignment.

2.1 GaAsN Alloy Bulk Layers

2.1.1 Lattice Constant

An incorporating N atom to GaAs is a new material that is GaAsN alloy. The added N atoms replace on As sites in GaAs crystal. According to the crystal structure of host GaAs matrix, crystal structure of dilute GaAsN alloy is still zinc-blend structure (cubic structure). Generally, it is expected that the physical properties of this alloy should be linearly dependence on the N concentration in the films and vary between the physical properties of GaAs and *c*-GaN. Thus, the material parameters (*P*), such as lattice constant and effective mass, of GaAsN alloy can be written as

$$P_{GaAs_{1-x}N} = x \cdot P_{c-GaN} + (1-x) \cdot P_{GaAs}, \qquad (2.1)$$

where x is the N concentration, $P_{GaAs_{1-x}N_x}$, P_{c-GaN} and P_{GaAs} are the material parameters of GaAsN, *c*-GaN and GaAs, respectively. The material parameters of GaAs and *c*-GaN are listed in Table 2.1. Thus the lattice constant of the GaAsN alloy can also be written as [17]

$$a_{GaAs_{1-x}N_x} = x \cdot a_{c-GaN} + (1-x) \cdot a_{GaAs}, \qquad (2.2)$$

where $a_{GaAs_{1-x}N_x}$, a_{c-GaN} and a_{GaAs} are lattice constants of GaAsN, *c*-GaN and GaAs, respectively. This equation is known as Vegard's law. In case of fully relaxed layer, the N concentration can be calculated from the lattice constant, by using Vegard's law. However, Vegard's law is no longer valid for the strained layers. It is because GaAsN grown on GaAs is under tensile strain. The lattice constant of the film in direction parallel to the interface (parallel lattice constant, $a_{//}$) will expand and the perpendicular lattice constant ($a_{\perp}$) will shrink. Thus, in this case, both lattice constants ($a_{\perp}$ and $a_{//}$) are considered to determine the N concentration in the tensile strained GaAsN layers on GaAs. The details of calculation are explained in Section 3.2.

2.1.2 Fundamental Electronic Band Structure

I. Anomalous Bandgap Bowing

It is well known that the bandgap energy of *c*-GaN (3.25 eV [18]) is larger than that of GaAs (1.424 eV [19]). According to Eq. (2.1), an increase in the bandgap energy was expected with incorporating N into GaAs. The studies of nitrogen containing III-V alloys are of great fundamental interest, because the addition of a few percent of nitrogen strongly decreases the bandgap energy as shown in Fig. 2.1 [9]. As a result, the bandgap energy of GaAsN is a parameter which deviates from the linear relation of Eq. (2.1). The bandgap energy of a conventional ternary III-V alloy

Table 2.1: Some material parameters of GaAs and *c*-GaN

parameters	GaAs	*c*-GaN
a(Å)	5.653 [19]	4.503 [20]
E_g (300) (eV)	1.424 [19]	3.25 [18]
E_V (eV)	1.46 [21]	-0.72 [21]
m^*_e	$0.067m_0$ [21]	$0.15m_0$ [18]
m^*_{lh}	$0.082m_0$ [22]	$0.19m_0$ [23]
C_{11}	11.88 [24]	26.4 [20]
C_{22}	5.38 [24]	15.3 [20]

C_{11} and C_{12} are in units of 10^{11} dyn/cm^2.

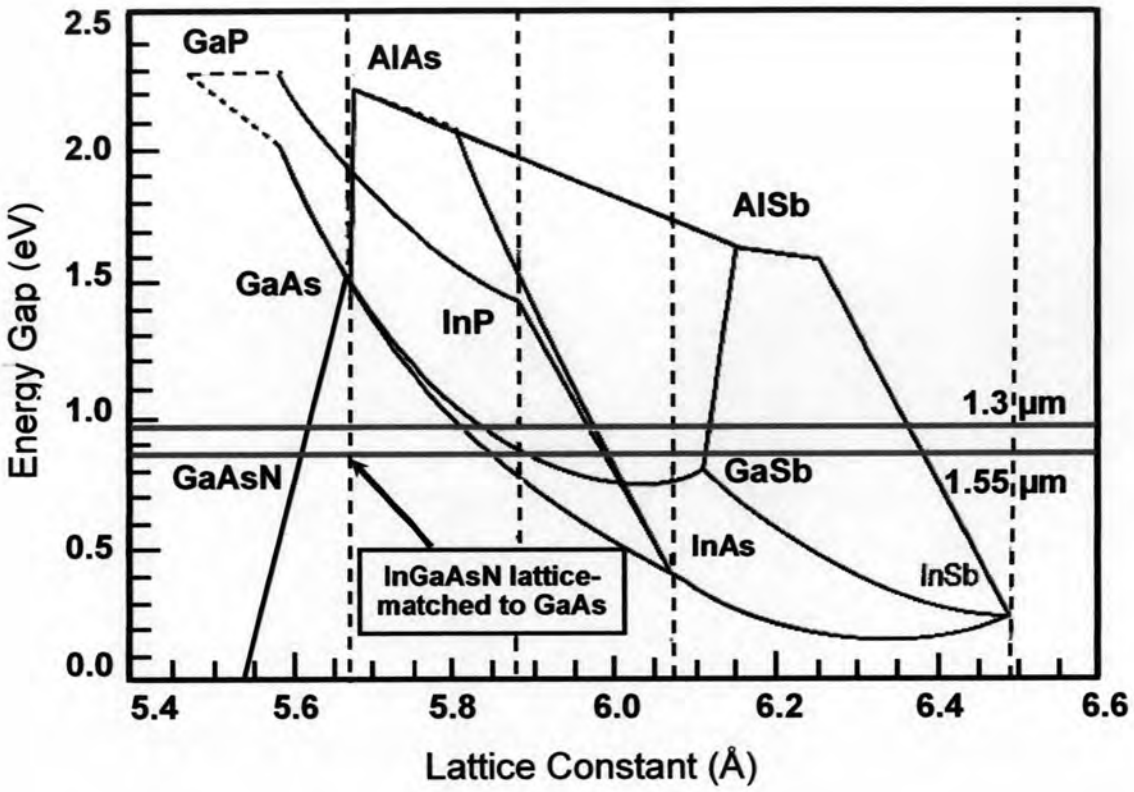

Figure 2.1: The relationship between the lattice constant and bandgap energy in III-V alloy semiconductors [9].

as well as GaAsN is usually represented by

$$E_g^{GaAsN} = x \cdot E_g^{c-GaN} + (1-x) \cdot E_g^{GaAs} - b \cdot x \cdot (1-x). \qquad (2.3)$$

The bowing parameter (b) is usually a small constant. In contrast, E_g of $GaAs_{1-x}N_x$ alloy is strongly red shifted with increasing N concentration (x), and b is very large (b = 16 eV for $x \leq 0.01$ and b = 26 eV for $x > 0.01$) [25]. In addition, more experimental data indicated that b varies with x [26]. This anomalous composition dependence of bandgap energy of $GaAs_{1-x}N_x$ is attracted to extend study electronic properties in this alloy. As a result, Eq. (2.3) is not suitable for prediction in bandgap energy of $GaAs_{1-x}N_x$ alloy.

II. Band Anticrossing Model

The following is a brief review of the present knowledge of the fundamental band structure of GaAsN alloy system. It has one model to explain the anomalous bandgap energy change in the $GaAs_{1-x}N_x$ alloy, namely a band anticrossing (BAC) model, which was proposed by Shan *et al.* [27]. The BAC model well represents the fundamental band structure of the dilute nitride GaAsN alloy. Thus, in this thesis, we used the BAC model to predict the bandgap energy in GaAsN alloy. The BAC model describes an interaction between the highly localized N-state and conduction-band-state. It was also used to explain the origin of the anomalous bandgap energy behavior or the large reduction of the bandgap energy, including pressure and temperature dependence, for the dilute III-V-nitride system as well as the highly mismatched systems. The added N atoms replacing on the As sites in the GaAs crystal contributes to the bandgap energy change according to

$$E_{\pm} = \frac{E_M + E_N \pm \sqrt{[E_M - E_N]^2 + 4V_{MN}^2 \cdot x}}{2}, \tag{2.4}$$

where x denotes N concentration and $E_{\pm}$ is the bandgap energy of the $GaAs_{1-x}N_x$ alloy. Where the top of valence band is taken as a reference energy level, E_M is the extended conduction band of GaAs, E_N is an impurity level due to incorporation of N atoms, which is assumed here to be located at 1.65 eV above the valence band of GaAs [28, 29]. V_{MN} is the coupling between the extended conduction band state (E_M) and the nitrogen state (E_N). The V_{MN} parameter is a fitting parameter and has a single constant value entire any alloy composition, for GaAsN alloy system V_{MN} = 2.7 eV [28, 29]. This model suggests that the interaction leads to a splitting of the conduction band into two subbands, E_+ and E_- levels representing the upper and lower lying subbands of the conduction band edge. The E_- level represents a large reduction of the fundamental bandgap energy. In addition, the BAC model can also be used to explain the electron effective mass (m^*_e) in the GaAsN alloy [28, 29]. The m^*_e is evaluated at the Brillouin zone center and is given by

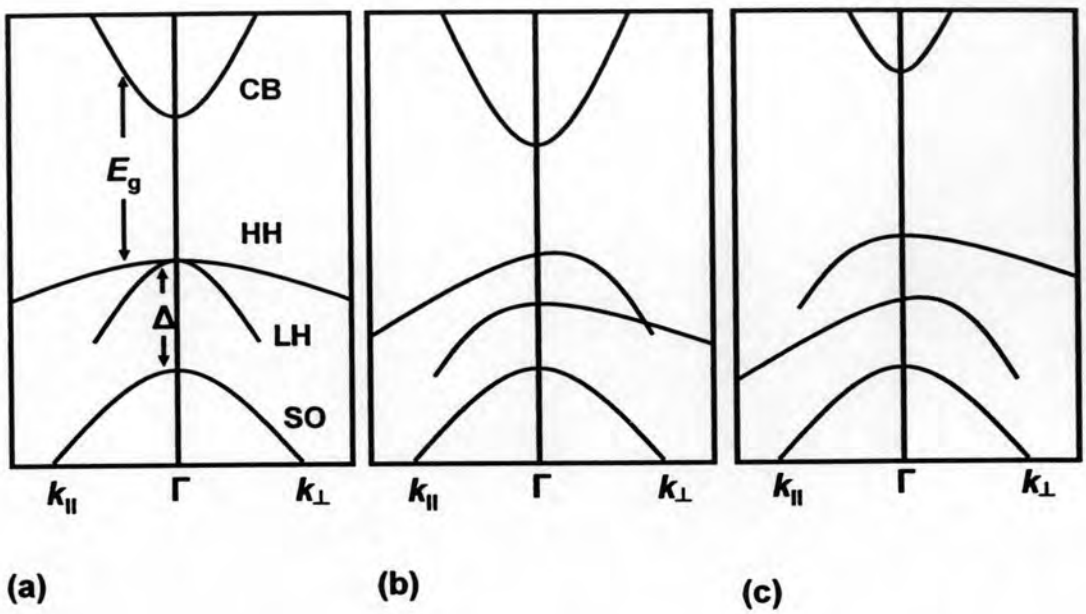

Figure 2.2: Schematic band representation in strained layers under (b) tensile and (c) compressive strain along with (a) the unstrained case [30].

$$m_e^* \approx \hbar^2 \left| \frac{k}{dE_-(k)/dk} \right|_{k=0}$$

$$= 2m_{e,GaAs}^* \Bigg/ \left[1 - \frac{E_M - E_N}{\sqrt{(E_M - E_N)^2 + 4V_{MN}^2 \cdot x}} \right]. \qquad (2.5)$$

The electron effective mass calculated in Eq. (2.5) increases rapidly with nitrogen concentration (x). Enhancing of m^*_e results in great improvement of the matching of the conduction and valence density of states. As a result, the efficiency of optical quality in the quantum well structures can be improved.

III. Strain-induced Bandgap

The growth of lattice-mismatched layer results in strain in the epilayer provided that the thickness of the epitaxial layer is below the critical thickness. If the lattice constant of the grown layer is smaller than that of the substrate, a tensile strain

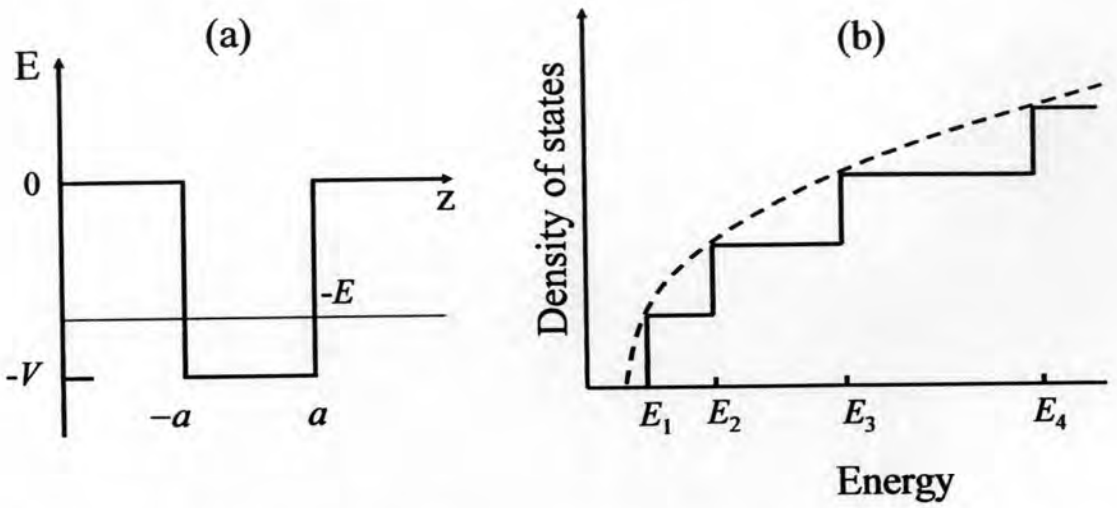

Figure 2.3: (a) Diagram of a finite square well potential and (b) density of states in quantum well and bulk (dashed line).

is introduced in the grown layer as in the case of the GaAsN epilayer on GaAs. Conversely, if the lattice constant of the grown layer is higher than that of the substrate, a compressive strain is presented in the grown layer as in the case of the InGaAs epilayer on GaAs. The schematic band diagrams of the two cases are depicted in Fig. 2.2 (b) and (c). When the strains are presented, the energy bands depend on the lattice structure. The strain affects on the degenerate valence band and splits the light-hole band from the heavy-hole band as shown in Fig. 2.2. The two bands move closer (apart) under the tensile (compressive) strain. As a result, the decrease (increase) of bandgap energy can be observed for tensile (compressive) strain.

We may now draw a conclusion on the observed bandgap energy of the tensile strained GaAsN layer on the GaAs substrate that it is a sum of both alloying bandgap energy and strain-induced energy shift. The bandgap energy in case of fully strained GaAsN layers exhibits smaller than that in case of the relaxed GaAsN layers.

2.2 GaAsN/GaAs Quantum Wells

2.2.1 DOS of 2-dimensional System

A quantum well (QW) structure is formed by one semiconductor material sandwiched between two higher bandgap energy layers with a very thin active region

in between as shown in Fig. 2.3 (a). In QW structure, the carriers are confined in one direction (growth direction), the carriers can move freely in two dimensions. The density of states (DOS) of the 2-dimentional system is independent of energy while DOS of the 3-dimentional system in the bulk layer increases with $\sqrt{E}$ as shown in Fig. 2.3 (b). The calculation for density of states can be found in several solid state text books [31, 32].

In a multiple quantum wells (MQWs) structure, the density of states can be modified from a single quantum well density of states according to [33]

$$\rho_{MQW}(E) = n \cdot \rho_{SQW}(E). \tag{2.6}$$

Where n are a number of periods. Because of the step like nature of 2-D density of states as shown in Fig. 2.3 (b), the efficiency of radiative recombination can be improved and is important to laser operation.

2.2.2 Quantum Confinement in Finite Quantum Well

Here, we apply the finite-depth single-square well model to calculate the confinement energies inside the well layer [34, 35]. The finite quantum well is illustrated in Fig. 2.3 (a). The conduction band edge of barrier material is at energy V higher than that of well material. The potential in the QWs structure in z-direction, is written as

$$V(z) = \begin{cases} -V, & |z| < a \\ 0, & |z| > a. \end{cases} \tag{2.7}$$

The effective-mass Schrödinger equation for particle of mass m_w^* in the well with well width of L_z is

$$-\frac{\hbar^2}{2m_w^*}\frac{d^2\varphi}{dz^2} + V(z)\varphi = E\varphi, \tag{2.8}$$

and

$$k_w^2 = \frac{2m_w^*(-|E| + |V|)}{\hbar^2}, \tag{2.9}$$

where φ is the envelope wave function for particle in the well, E is the energy measured with respect to the top of the barrier and V is the barrier height energy. In the barrier material, the effective-mass Schrödinger equation is

$$-\frac{\hbar^2}{2m_b^*}\frac{d^2\varphi}{dz^2} = E\varphi. \tag{2.10}$$

Thus
$$k_b^2 = \frac{2m_b^*|E|}{\hbar^2}, \tag{2.11}$$

where m_b^* is the effective mass in the barrier, E is again the energy measured with respect to the top of the barrier and φ is the envelope wave function for particle in the barrier. The boundary condition at $z = \pm a$ that φ and $(1/m^*)d\varphi/dz$ are continuous [34, 35]. We obtain

$$k_b m_w^* = k_w m_b^* \tan k_w a. \tag{2.12}$$

Equation (2.12) can be solved numerically or graphically and the solution gives information about the lowest quantized energy state E_1 which directs the optical properties of the quantum well structures. From Eq. (2.12), a is a half of well width L_z and $\hbar = \frac{h}{2\pi}$, h is Plank's constant.

2.2.3 Effective Masses in the Wells

In order to calculate the quantized energy E_1 in the wells, the effective mass of particle in the well layers is a required consideration. The recombination process inside the well layer is originated from the excitonic recombination. For the tensile strained GaAsN well layer, the energy state of the light-hole is higher than that of the heavy-hole. As a consequence, the effective mass of particle (exciton) inside the well can be determined by reduced masses between the electron effective mass (m^*_e) and light-hole effective mass (m^*_{lh}), which are evaluated at the Brillouin zone center. The

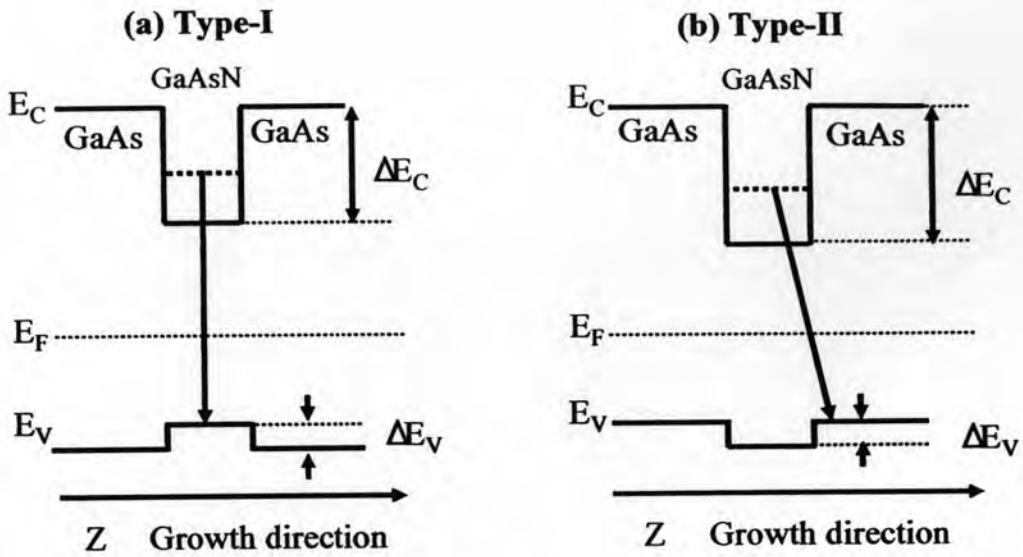

Figure 2.4: Schematic band diagrams of the quantum structures with (a) type-I and (b) type-II band alignment and their expected properties.

value of m^*_e, is estimated from the BAC model as indicated in Eq. (2.5). On the other hand, the value of m^*_{lh} for $GaAs_{1-x}N_x$ can be approximately determined using a linear interpolation between the values of m^*_{lh} of GaAs and *c*-GaN. The lists of m^*_e and m^*_{lh} for GaAs and *c*-GaN are summarized in Table 2.1.

2.2.4 Band Alignment of GaAsN/GaAs Heterostructure

Here, we focus on the fundamental types of the band alignment of the GaAsN/GaAs QW structure. Figure 2.4 shows promising types of band alignment of the GaAsN/GaAs QWs, namely (a) a type-I and (b) a type-II QWs structures. To know the optical transition energy in GaAsN/GaAs QWs, we have demonstrated here a possible fundamental type of band alignment of the GaAsN/GaAs QWs. To establish the band alignment, the valence band offset (ΔE_V) is a first required consideration. Sakai *et al.* theoretically predicted that bowing of the valence band of the dilute $GaAs_{1-x}N_x$ alloy is negligible [36]. Thus, in our study, the natural valence band (E_V) alignment of the $GaAs_{1-x}N_x$ alloy was approximately evaluated using a

linear interpolation between the values of E_V of GaAs and *c*-GaN (see in Table 2.1). As a result, the value of ΔE_V of the $GaAs_{1-x}N_x$/GaAs QW structure can be calculated by setting the E_V alignment of GaAs as a reference energy level. The value of ΔE_V of the $GaAs_{1-x}N_x$/GaAs QW structure can be expressed as

$$\Delta E_v = -2.18x. \tag{2.13}$$

Along with Eq. (2.13), we found that $GaAs_{1-x}N_x$/GaAs heterostructure have a negative valence band offset. Therefore, the fundamental type of the band alignment of the $GaAs_{1-x}N_x$/GaAs QWs structure should be type-II band lineup as shown in Fig. 2.4 (b).

It is noted that, for the strained GaAsN/GaAs QWs, the energy band especially the valence band is affected not only by quantum confinement effects but also by strain. In GaAsN/GaAs QW system, we concern only in the tensile strain, the energy state of the light-hole band is higher than that of the heavy-hole band. Thus, the effective mass of exciton in the GaAsN well layer corresponds to interaction between the electrons effective mass and light-hole effective mass. The splitting of the valence bands results in reduction of the effective hole mass and greatly enhances the matching of the valence and conduction band density of states. Hence, the efficiency of performance of semiconductor lasers is also improved by using a strained quantum well as an active layer.